Optimal Process Operation for the Production of Linear Polyethylene Resins with Tailored Molecular Weight Distribution

K. V. Pontes

Industrial Engineering Program (PEI)—Universidade Federal da Bahia—R. Aristides Novis No 2, Federação, Salvador-BA, Brazil

AVT—Process Systems Engineering, RWTH Aachen University, Turmstr. 46, 52064 Aachen, Germany

M. Embiruçu

Industrial Engineering Program (PEI)—Universidade Federal da Bahia—R. Aristides Novis No 2, Federação, Salvador-BA, Brazil

R. Maciel

Laboratory of Optimization, Design and Advanced Control (Lopca)—Campinas State University—Cidade Universitária Zeferino Vaz, Caixa Postal 1170, Campinas-SP, Brazil

A. Hartwich

AVT—Process Systems Engineering, RWTH Aachen University, Turmstr. 46, 52064 Aachen, Germany

German Research School for Simulation Sciences GmbH, 52064 Aachen, Germany

W. Marquardt

AVT—Process Systems Engineering, RWTH Aachen University, Turmstr. 46, 52064 Aachen, Germany

An optimization model is presented to determine optimal operating policies for tailoring high density polyethylene in a continuous polymerization process. Shaping the whole molecular weight distribution (MWD) by adopting an appropriate choice of operating conditions is of great interest when designing new polymers or when improving quality. The continuous tubular and stirred tank reactors are modeled in steady state by a set of differential-algebraic equations with the spatial coordinate as independent variable. A novel formulation of the optimization problem is introduced. It comprises a multi-stage optimization model with differential-algebraic equality constraints along the process path and inequality end-point constraints on product quality. The resulting optimal control problem is solved at high computational efficiency by means of a shooting method. The results show the efficiency of the proposed approach and the benefit of predicting and controlling the complete MWD as well as the interplay between operating conditions and polymer properties. © 2010 American Institute of Chemical Engineers AIChE J, 57: 2149–2163, 2011

Keywords: mathematical modeling, multi-stage optimization, polymerization, reaction engineering, polyethylene, molecular weight distribution

Introduction

Polymer materials are present in everyday life, in segments such as packing, transport, and construction. Their end-use properties depend heavily on the operating conditions under which the polymer is synthesized. In industrial practice, polymerization processes are usually operated according to a predetermined recipe, which reflects available chemical knowledge and the practical experience of the process operators. Often, the processes are operated under suboptimal conditions due to the lack of a systematic method for determining the best operating policies. Today, process models as well as optimization tools are available and they provide the foundation for a systematic process and product quality improvement. As a result, there is considerable interest within the polymer industry to develop optimal operating policies that will result in the production of polymers with desired molecular properties.

According to Kiparissides,[1] there are two classes of optimization problems for polymerization reactors: steady-state optimization, which deals with the selection of the best (optimum) time invariant controls such that the molecular properties attain certain desired values; and dynamic optimization (or optimal control), which refers to the determination of optimal control trajectories to move a polymer reactor from its initial to a desired final state. The former is usually related to the steady-state operation of continuous polymer reactors while the latter is concerned with the dynamic operation of batch and semibatch reactors as well as with start-up, shut-down, and grade transition policies for continuous polymerization processes. The focus of the present article is the optimal steady-state operation of a complex reactor configuration comprising a series of continuous tubular and stirred tank reactors to meet a specified polymer at the lowest production cost.

Polymer quality is usually specified in terms of end use properties such as stiffness, melting temperature, and crystallization temperature. Some attempts have been made to correlate such polymer end-use properties with lumped properties which can easily be measured in a polymer production plant. A typical example is given by the melt index (MI).[2,3] However, rheological and processing properties might differ significantly if the molecular weight distribution (MWD) is skewed and shows high concentrations of high or low molecular weight fractions. In particular, Ariawan et al.[4] show that the rheological properties of the polymer are affected by the complete MWD. They conclude that the extensional and elastic properties are very much dependent on the distribution tail, referring to molecules with large molecular weight. Consequently, several authors developed correlations between polymer properties and the whole MWD. For example, Hinchliffe et al.[5] propose a methodology to correlate the MI, the shear thinning ratio and the dart impact with selected bins of the MWD. Furthermore, Nele et al.[6] successfully predict the MI from the entire MWD using convolution of the MWD and a kernel function. More recently, Zahedi et al.[7] have used spline functions to correlate flow properties of the polymer melt with the entire MWD. Motivated by these findings, the full MWD is used in this work as the target quality property to be met by optimal operation of the polymer production plant in steady state.

There have been many attempts to determine optimal operating conditions of polymerization processes to produce polymers with target average molecular weight and polydispersity. Most of the research considered the polymerization of methyl methacrylate (MMA) in batch reactors.[8–12] However, the first moments of the MWD and average properties are in many cases insufficient to describe polymer end-use properties satisfactorily.[4] Despite the importance of predicting the full MWD, as discussed previously, only few papers report on determining optimal operating policies for polymer production with a target MWD. Crowley and Choi[13] obtain optimal temperature trajectories to control the MWD of MMA produced in a batch reactor, using the method of finite molecular weight moments for capturing MWD.[14] In another contribution,[15] the same authors determine optimal temperature and initiator concentration policies to target the tensile strength of the polystyrene produced in a batch suspension reactor. Sayer et al.[16] compute the optimal monomer and chain transfer feed profiles for MMA batch copolymerization to produce a polymer with a specified copolymer composition and MWD. Kiparissides et al.[17] propose a temperature control scheme for free radical polymerization of MMA in a batch reactor. An optimization step ensures the production of a polymer with target properties which include not only the average molecular weights but also the complete MWD. More recently, Kiparissides and coworkers[18] use an optimization model to determine the optimal temperature profile that produces the target MWD of MMA in minimum batch time. Vicente et al.[19] target MWD, copolymer composition and final monomer concentration in a semibatch emulsion polymerization of MMA/n-butylacrylate and compare the optimization results with experiments in a pilot plant. While all the works discussed so far report on (semi)batch polymerization processes, Asteasuain et al.[20] consider optimal steady-state operation of a living polymerization of styrene in a tubular reactor with a targeted MWD. In a second publication,[21] these authors also explore the optimization model to determine operating conditions resulting in a multimodal MWD.

Brandolin and coworkers have addressed the computation of optimal operating policies to achieve target product properties in continuous polyethylene production. This group studied a continuous high pressure tubular reactor for the production of low density polyethylene (LDPE). Brandolin et al.[22] derive optimal steady-state operating points (temperature and initiator concentration) to attain a specific number average molecular weight, polydispersity and weight average branch point number in the effluent product. Asteasuain et al.[23] studied start-up and shutdown strategies to maximize outlet conversion, while satisfying the desired number average molecular weight and transition time. Cervantes et al.[24] have extended the dynamic reactor model to the entire plant to study optimal grade transitions for LDPE production. This optimization criterion tries to minimize copolymer content in the recycle stream as well as transition time. In these articles, no attempt has been made to tailor the complete MWD. In their latest work, however, Asteasuain and Brandolin[25] focus on the optimization of an LDPE tubular reactor to maximize conversion while targeting the entire MWD through constraints using a steady-state model. They predict bimodal MWD when feeding monomer and chain transfer agent at a fixed lateral injection point of the multi-stage tubular reactor with counter-currently cooling. The
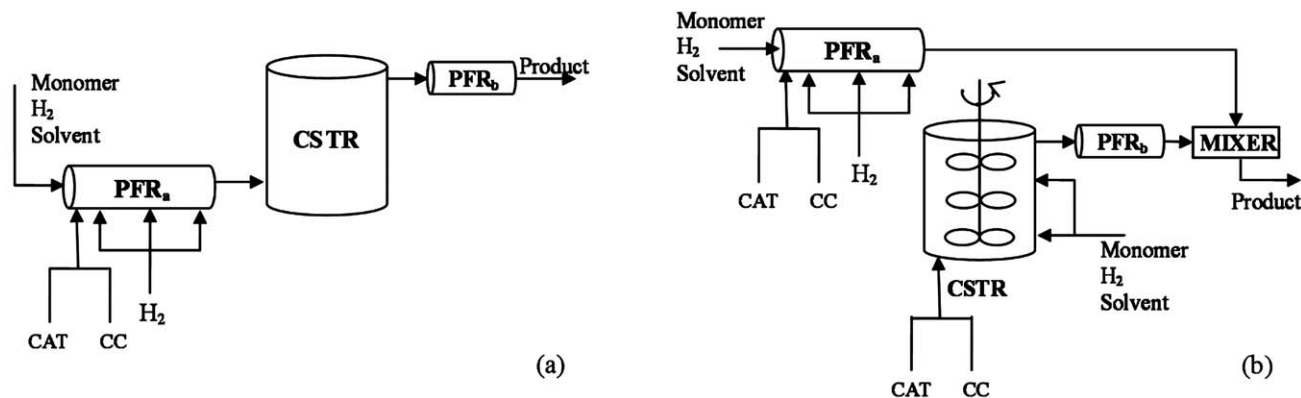
Figure 1. Typical reactor configuration: series (a) and parallel (b).

optimization problem has been solved in gPROMS after a spatial discretization of the differential-algebraic model to handle the multi-point boundary conditions. More recently Zavala and Biegler[26] optimize the operation of a multi-zone tubular reactor for the production of LDPE with target melt-index and density for a sequence of decaying heat transfer coefficients. They also employ a spatially discretized formulation of the steady-state reactor model to obtain a large-scale nonlinear programming problem. These authors do not attempt to tailor the complete MWD of the resin.

Kiparissides' group also studied the continuous production of LDPE in tubular reactor for optimization and control purposes.[27,28] The gas phase and slurry ethylene continuous polymerizations were also object of studies approaching the optimal control of grade transitions.[29–32] Despite the significant amount of work on optimization of polyethylene reactor, to the authors' knowledge, optimal operating policies for a continuous solution polymerization in a complex reactor configuration consisting of tubular and stirred tank reactors has not yet been treated adequately in literature.

Our previous work[33] has suggested a new formulation of an optimization problem to find optimal steady-state operating conditions of a continuous multi-reactor polymerization process that produces a tailored polymer with a targeted MI and stress exponent (SE). In contrast to the work of other research groups reviewed above, we have considered ethylene polymerization in solution using a Ziegler-Natta catalyst in a complex configuration of continuous stirred tank (CSTR) and plug flow reactors (PFR). The optimization problem formulation relies on a steady-state multi-stage model with the spatial coordinate as independent variable which—together with product quality specifications—constitute the constraints of an optimization problem with economic objective. The multi-stage optimal control problem reveals discontinuities with respect to the spatial coordinate due to different types of reactors and lateral feed injections points which are themselves decisions in the optimization.

This article presents an extension of our previous work focusing on the production of tailored linear polyethylene, the quality of which is not only specified through lumped quality properties such as MI and SE but through the complete MWD. This detailed treatment of the quality specification is of great industrial importance, because of the complex trade-off between polymer properties—ultimately determined by

the MWD—and the economics of production. The polymerization model is complex not only due to its multi-stage and spatially distributed character but also due to the MWD used to predict polymer quality. The original contribution of this article is the efficient and accurate solution of this complex optimization problem using a multi-stage optimal control problem formulation in the spatial coordinate and single shooting rather than spatial discretization for its solution. The novel numerical approach proposed here overcomes some problems reported in previous literature, even for problems of lower complexity. Furthermore, we show that polyethylene products with very different MWD and average polymer properties can be produced economically in the same plant under different process configurations and at different operating points. Therefore, the second original contribution of the article constitutes of a systematic methodology to support product design engineers and plant operators to develop and produce new resins or existing resins of improved quality, which is specified by the complete MWD.

The article is structured as follows. First, the polymerization process is described. Then, the mathematical models of the process and the polymer properties as well as the method for computing the MWD are presented. In the next section, the optimization problem is formulated and the solution method is discussed and compared with previously suggested methods. Then, the results of several optimization runs are discussed to illustrate the applicability, potential and efficiency of the proposed modelling and solution procedure. Finally, the article is concluded.

Process Description and Mathematical Model

The polymerization takes place in a series of PFR and CSTR that can be arranged in different configurations to produce different linear polyethylene grades. Two possible configurations are illustrated in Figure 1, the series (left) and the parallel (right) configurations. In the series configuration, the stirrer of the CSTR is switched off such that it operates as a PFR with a large diameter resulting in some degree of back-mixing due to axial dispersion. Hydrogen, the chain transfer agent, can be injected not only together with the main feed but also at several points along the first tubular reactor to control the MWD. To allow for J mass injections points at positions to be determined as part of the optimization, the

first PFR is divided into J segments with PFR characteristics, where the starting point of compartment j is located at the lateral mass injection points. When operating the parallel configuration, the main feed to the CSTR can be split so that part of it feeds the top of the reactor in addition to the feed at the bottom.

A detailed description of the process and the mathematical model is beyond the scope of this article. The appendix briefly summarizes the kinetic mechanism, the model equations and the polymer property models. For further details on model development, we refer to Pontes et al.[33] and Embiruçu et al.[34–39] Model parameters, including kinetic and physical properties constants, have been validated with experimental data from an industrial polymerization process in their work. MI and SE are used to infer the average molecular weight and the polydispersity, respectively.

In our previous work[33] on optimal operating policies, only average properties of the MWD have been considered, requiring only the prediction of the first three moments to describe product quality. In contrast, the present study focuses on targeting the complete MWD to enable a more detailed specification of the target polymer quality. Therefore, equations for the dead polymer concentration are also required. The mass balances for the dead polymer in the CSTR and PFR are given by[34,40]

$$\frac{dU_{p,j}}{dz_j} = \frac{U_{p,j}}{\rho_j} \cdot \frac{d\rho_j}{dz_j} + r_{U_p} \cdot \frac{A \cdot \rho_j}{W_j},$$
$$z_j \in (0, l_j], j = 1, \ldots, J+1, p = 2, \ldots, \infty, \quad (1)$$

$$\frac{W_{r-1} \cdot U_{p,r-1}}{\rho_{r-1}} + \frac{FZ_r \cdot U_{p,r}}{\rho_{FZ_r}} + \frac{B_{r+1} \cdot U_{p,r+1}}{\rho_{r+1}}$$
$$- \frac{(B_r + W_r) \cdot U_{p,r}}{\rho_r} + V_r \cdot r_{U_p} = 0, r = 1, \ldots, R. \quad (2)$$

z is the axial coordinate, l_j is the length of segment j, W_j, B_j, and FZ_j are mass flow rates (kg/s), U_p is the concentration of dead polymer with length p (kmol/m^3), r_{U_p} is the reaction rate of dead polymer with p monomer units (kmol/s·m^3), A is the cross-sectional area (m^2), ρ is the density of the mixture (kg/m^3), V_r is the volume of an ideal CSTR segment (m^3) and J and R are the number of PFR and CSTR segments, respectively. The reaction rate of the dead polymer is given by[40]

$$r_{U_p} = P_1 \cdot \left(\frac{f_{cp}}{k_p \cdot M} + 1 \right)^{1-p} \cdot f_{cp}, \quad p = 2, \ldots, \infty, \quad (3)$$

$$f_{cp} = (k_{fm} + k_{tm}) \cdot M + k_{fh} \cdot H_2^{ofh} + k_{th} \cdot H_2^{oth}$$
$$+ k_{fcc} \cdot CC^{ofcc} + k_{tcc} \cdot CC^{otcc} + k_f + k_t, \quad (4)$$

where P_p is the concentration of live polymer with length p. M, H$_2$, and CC are the monomer, hydrogen, and co-catalyst concentrations, k is the reaction rate, the subscripts f and t refer to transfer and termination reactions, the indices m, h, and CC refer to monomer, hydrogen, and co-catalyst and the exponents ofh, oth, ofcc, and otcc denote the order of transfer and termination reactions with hydrogen and co-catalyst.

Since it is impossible to directly solve an infinite number of mass balance equations for the dead polymer (Eqs. 1 and 2), one of the established methods has to be employed to approximate the complete MWD. Among others, these methods include the generating function,[41] the finite molecular weight moments,[13] the differentiation of the cumulative MWD[40] and the orthogonal collocation method.[16–17] In this work, orthogonal collocation[42] in the setting of a discrete weighted-residual method is used to compute an approximation of the MWD.[43–44] The method assumes that the concentration of the dead polymer chains (U_p) may be approximated by

$$U_p \approx \tilde{U}(p) = \sum_{k=1}^{N} b_k \cdot \phi_k(p), \quad (5)$$

on the chain-length domain P, i.e., comprising a finite number of chain lengths $p = 2, \ldots, P$, where ϕ_k is a known set of N linearly independent polynomial functions. The coefficients b_k have to be determined to find the best approximation. If ϕ_k is a Lagrange polynomial, the coefficients b_k turn out to be the values of the function $\tilde{U}(p)$ at the collocation points p_k, $k = 1, \ldots, N$. While the size of the original problem scales with the number of elements in the domain P, the reduced model scales with N. Therefore, Eqs. 1 and 2 have to be solved at N collocation points to result in

$$\frac{d\tilde{U}(p_k, z)_j}{dz_j} = \frac{\tilde{U}(p_k, z)_j}{\rho_j} \cdot \frac{d\rho_j}{dz_j}$$
$$+ P_1 \cdot (w+1)^{1-p_k} \cdot f_{cP} \cdot \frac{A \cdot \rho_j}{W_j}, k = 1, \ldots, N, \quad (6)$$

$$\frac{W_{r-1} \cdot \tilde{U}(p_k)_{r-1}}{\rho_{r-1}} + \frac{FZ_r \cdot \tilde{U}(p_k)_r}{\rho_r} + \frac{B_{r+1} \cdot \tilde{U}(p_k)_{r+1}}{\rho_{r+1}}$$
$$- \frac{(B_r + W_r) \cdot \tilde{U}(p_k)_r}{\rho_r} + V_r \cdot P_1 \cdot (w+1)^{1-p_k} \cdot f_{cP}. \quad (7)$$

The approximate MWD at the collocation point p_k can then be obtained from[17,20,45]

$$wd_k = p_k \cdot \tilde{U}(p_k), \quad k = 1, \ldots, N, \quad (8)$$

where wd_k is the concentration of monomer incorporated to the polymer with chain length p_k.

The total chain length domain P is selected as 40,000 monomer units for convenience.[46] This finite domain is divided into dim finite elements based on a uniform logarithmic grid.[40] The collocation points are then calculated within each interval based on Hahn polynomials of order nh.[17] Different combinations of dim and nh were tested to evaluate the approximation quality. The best set of parameters has been determined as $dim = 10$ and $nh = 2$ to result in $N = 21$ collocation points. A higher number of points yields almost the same MWD, as shown in Figure 2, but at higher computational effort, while a lower number does not provide results at the desired level of accuracy.

In addition to the MWD, the moments of the distribution are computed to calculate the average molecular weights and the polydispersity. Therefore, equations for the dead polymer moments of order zero, one, and two (λ_0, λ_1, λ_2) have been added to the mass balance model.

In an industrial setting, PE grade specifications are generally quoted in terms of MWD, MI, density, and some measure of MWD broadness, rather than average molecular weight and comonomer content. Hence, relationships between MI and average molecular weight and between SE and polydispersity have been incorporated into the models.
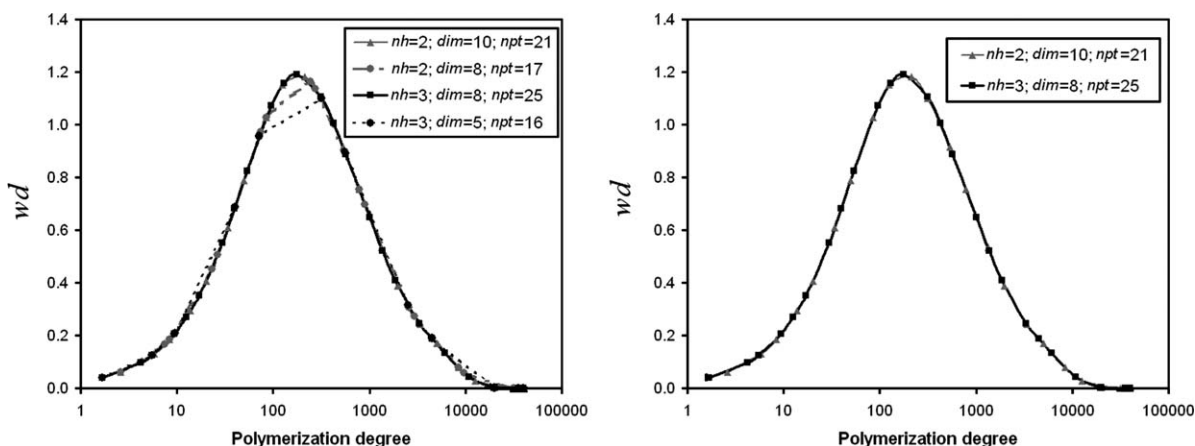
Figure 2. Comparison between different sets of *nh* and *dim*.

The MI measures the weight average molecular weight with an inverse relationship, that is, a higher MI corresponds to a lower molecular weight. On the other hand, the SE is a measure for MWD broadness, e.g., a higher SE refers to a broader MWD and hence a higher polydispersity.

Optimization Problem Formulation

The objective of optimization is supposed to reflect some economic criterion. In batch polymerization, often batch time is minimized or monomer conversion is maximized while constraining the target average molecular weights and polydispersity.[8,9] Another very common approach relies on an objective function which combines a number of performance measures with appropriate weighting factors chosen a priori.[10,11] However, the choice of weightings is not always easy because it lacks a transparent conflict resolution. Alternatively, the weighted sum of squares of the deviation of desired monomer conversion and polymer properties from their specified values has been minimized.[12,16,17] None of these contributions attempted to target the economical performance of the process directly.

Only a few authors employed a truly economic objective in the optimization, accounting for reactant cost or revenue for example. O'Driscoll and Ponnuswamy,[47] Oliveira et al.,[48] and Tieu et al.[49] consider the initiator cost together with the batch time in a multiobjective optimization with constraints on polydispersity, number average molecular weight and copolymer composition (when it applies). Zavala and Biegler[26] show that adding polymer production to the objective function improves the economic performance of the process.

When the optimization objective only refers to polymer properties, economically sub-optimal operating conditions may be found, since often several operating conditions yield resins with similar properties. Furthermore, though maximum conversion or minimum batch time are somehow related to profit, they do not ensure optimal economic operation. Therefore, in the present approach we maximize an economic profit function given by

$$\Phi = a \cdot W_{PE} - (b_M \cdot W_M + b_H \cdot W_H + b_{CAT} \cdot W_{CAT} + b_{CC} \cdot W_{CC} + b_S \cdot W_S), \quad (9)$$

where a is the polyethylene sales price (€/kg), b_j represents the cost (€/kg) of raw material j, W_j is a mass flow rate (kg/s) and the subscripts PE, M, H, CAT, CC, and S denote polyethylene, monomer, hydrogen, catalyst, co-catalyst, and solvent, respectively. In industrial practice, the market might demand certain amounts of polymer which can be achieved by constraining the polymer production rate in the optimization problem. Maximization of an economic profit function, constrained to market demand, leads to optimal conditions with higher profit than in industrial practice.[33] Therefore, better process performance may be achieved if profit is used as the optimization criterion, instead of using polymer production, conversion or polymer properties in the objective function.

The decision variables for the series and the parallel process configurations (*s*: series; *p*: parallel), determined by a design of experiment approach,[50] are

$$\mathbf{u}_s = \begin{bmatrix} M_T & H_{2,0,T} & CAT_T & T_{in,T} & H_{2,1,T} & z_{1,T} & W_{t,T} & P_{in,T} \end{bmatrix}, \quad (10)$$

$$\mathbf{u}_p = \begin{bmatrix} M_C & H_{2,0,C} & CAT_C & W_{s,C} & W_{t,C} & P_{in,C} & \mathbf{u}_s \end{bmatrix}, \quad (11)$$

where M, $H_{2,0}$, and CAT are monomer, hydrogen, and catalyst inlet concentrations, respectively, T_{in} is the inlet temperature, W_t the total mass flow rate, P_{in} the inlet pressure, W_s the side feed to the CSTR, z_1 the lateral hydrogen injection point, $H_{2,1}$ is the concentration at that point and subscripts C and T refer to CSTR and PFR$_a$, respectively. The number of lateral injection points is (pragmatically) fixed to one a priori, such that no discrete variables have to be considered in the optimization. The total length of PFR$_a$ is held constant.[33]

The desired polymer properties are specified by equality and inequality constraints at the outlet of the last reactor in the sequence. The target MWD may be specified by defining n bounds for wd_i, $i = 1,...,n$, $n \leq N$. The vector of quality constraints at the outlet of PFR$_b$ is

$$\mathbf{h} = [MI \quad SE \quad \mathbf{wd}]. \quad (12)$$

The detailed formulation of the optimization problem is given in our previous work[33] and is not repeated here. The stationary mathematical model of the CSTR consists only of algebraic equations, whereas the PFR model is represented by

a differential-algebraic system with the axial coordinate z as independent variable. A multi-stage model with discontinuities along the spatial coordinates results due to the transitions from one reactor to the other and due to lateral hydrogen injection along the flow path in the PFR_a (Figure 1). This multi-stage model is solved by integrating along the axial coordinate z. Every PFR model is associated with a finite length spatial interval while the CSTR models are associated with a spatial interval with zero length as no differential equations are involved. Hence, the CSTR model becomes part of the stage transition (or the initial) conditions. More precisely, the CSTR model enters the initial conditions of PFR_b for both configurations (Figure 1).

The multi-stage optimization problem for the series configuration (Figure 1a) reads as

$$\max_{\mathbf{u}_k} \Phi \tag{13}$$

s.t

$$\dot{\mathbf{x}}_k = \mathbf{f}_k(\mathbf{x}_k, \mathbf{y}_k, \mathbf{u}_k, \mathbf{p}, z), z \in [z_{k-1}, z_k], k = 1, .., J, J+2, \tag{13a}$$

$$0 = \mathbf{g}_k(\mathbf{x}_k, \mathbf{y}_k, \mathbf{u}_k, \mathbf{p}, z), z \in [z_{k-1}, z_k], k = 1, ..., J, J+2, \tag{13b}$$

$$0 = \mathbf{x}_1(z_0) - \mathbf{x}_0, \tag{13c}$$

$$\mathbf{J}_k(\dot{\mathbf{x}}_k, \mathbf{x}_k, \mathbf{y}_k, \mathbf{u}_k, \dot{\mathbf{x}}_{k-1}, \mathbf{x}_{k-1}, \mathbf{y}_{k-1}, \mathbf{u}_{k-1}, \mathbf{p}, z) = \mathbf{0}, k = 2, ..., J+2, \tag{13d}$$

$$\mathbf{u}_{LB} \le \mathbf{u}_k \le \mathbf{u}_{UB}, \tag{13e}$$

$$\mathbf{h}_{LB} \le \mathbf{h} \le \mathbf{h}_{UB}, z = z_f, \tag{13f}$$

where $\mathbf{x}$ and $\dot{\mathbf{x}}$ are differential state variables and their derivates with respect to the spatial coordinate z, $\mathbf{y}$ the algebraic state variables, $\mathbf{u}$ the decision variables, and $\mathbf{p}$ the invariant parameters. Equation 13c defines the initial conditions of the first stage, i.e. the first segment of PFR_a. For the following PFR segments $k = 2,...,J$ and $k = J + 2$ the initial conditions are determined by the stage transition conditions (13d). The steady-state model of the CSTR relies only on one compartment and thus does not comprise any differential equations such that the CSTR model equations can be incorporated into the mapping conditions (13d) for $k = J + 1$. Here, the partial vectors $\mathbf{u}_k$ are formed by appropriate subsets of $\mathbf{u}_s$ (cf., Eq. 10). $\mathbf{h}$ are the constraints at the reactor outlet (cf., Eq. 12).

In the parallel configuration (Figure 1b), if one lateral hydrogen injection point is used, the resulting two segments of PFR_a define two stages which are represented by $\xi_T = \{1,2\}$. Note that any other number of injection points can be accommodated easily. These stages run in parallel with two other stages denoted by $\xi_C = \{1,2\}$, i.e., the CSTR and the PFR_b. The mixer constitutes an additional stage $\xi_M = \{3\}$ which consists only of algebraic equations. The multi-stage optimal control problem for the parallel configuration is therefore mathematically formulated as:

$$\max_{\mathbf{u}_1} \Phi \tag{14}$$

s.t.

$$\dot{\mathbf{x}}_k = \mathbf{f}_k(\mathbf{x}_k, \mathbf{y}_k, \mathbf{u}_k, \mathbf{p}, z), z \in [z_{k-1}, z_k], k \in \xi_T \vee \xi_C \backslash \{1\}, \tag{14a}$$

$$0 = \mathbf{g}_k(\mathbf{x}_k, \mathbf{y}_k, \mathbf{u}_k, \mathbf{p}, z), z \in [z_{k-1}, z_k], k \in \xi_T \vee \xi_C \backslash \{1\}, \tag{14b}$$

$$0 = \mathbf{x}_1(z_0) - \mathbf{x}_0, \tag{14c}$$

$$\mathbf{J}_k(\dot{\mathbf{x}}_k, \mathbf{x}_k, \mathbf{y}_k, \mathbf{u}_k, \dot{\mathbf{x}}_{k-1}, \mathbf{x}_{k-1}, \mathbf{y}_{k-1}, \mathbf{u}_{k-1}, \mathbf{p}, z) = \mathbf{0},$$
$$k \in \xi_T \vee \xi_C \vee \xi_M, \tag{14d}$$

$$\mathbf{u}_{LB} \le \mathbf{u}_k \le \mathbf{u}_{UB}, \tag{14e}$$

$$\mathbf{h}_{LB} \le \mathbf{h} \le \mathbf{h}_{UB}, z = z_f, \tag{14f}$$

where $\mathbf{u}_k$ are appropriate subsets of $\mathbf{u}_p$ in Eq. 11 and $\mathbf{J}_k$ is the set of algebraic equations that maps the outlet conditions of stage k-1 to the initial conditions of stage k. Particularly when $k \in \xi_C \backslash \{2\}$ or $k = 3$, $\mathbf{J}_k$ is the set of algebraic equations for the CSTR and the mixer. Further details on the formulation of the optimization problem can be found elsewhere.[33]

When computing the complete MWD, a more complex optimization model has to be solved due to the larger number of differential equations and mapping conditions that arise from the mass balances. If N is the number of collocation points, N differential equations such as (6) have to be solved additionally for each PFR segment, hence $(J + 1) \cdot N$ equations in total. The CSTR model adds in turn N algebraic equations such as (7). The same holds true for the mixer model used in the parallel configuration. Furthermore, for each stage transition additional N mapping conditions (Eqs. 13d and 14d) have to be satisfied. In addition to these differential-algebraic constraints, end-point inequality constraints are formulated to target the desired polymer properties at the reactor outlet. The solution of the multi-stage optimization problem requires a robust and efficient algorithm if the model predicts the complete MWD.

One possibility to specify a desired MWD is to define the polymer distribution wd_k, $k = 1,...,N$ at every degree of polymerization represented by a collocation point. This would result in N additional constraint (Eqs. 13f and 14f) at the reactor outlet. Our results show however, that the desired MWD can be satisfactorily predicted and hence specified using, for example, only four collocation points. A more accurate specification prediction can be achieved if the distribution's average and dispersion are additionally set. We will show below how different constraint sets can be used to specify tails at higher chain lengths and even bimodal distributions.

The numerical solution of the optimization problem is carried out with DyOS, a dynamic optimization software developed and maintained at AVT—Process Systems Engineering, RWTH Aachen University (Germany).[51–53]

This dynamic optimization software allows for a robust multi-stage formulation and solution. The multi-stage formulation, through its stage transitions, allows the lateral injection points to be modeled as true impulses. Instead of spatially discretizing the differential-algebraic equations on a fixed grid,[25–26] the approach proposed here consists on integrating a dynamic model whose independent variable is the spatial coordinate, as mentioned previously. Each stage is then integrated along a finite length spatial interval so that

Table 1. Computational Efficiency*

	Series Configuration						Parallel Configuration						
	1a	1b	1c	2a	2b	2c	3a	3b	3c	3d	4a	4b	4c
Inequality constraints	8	12	16	6	8	8	4	4	4	4	8	4	6
NLP iterations	190	130	178	157	139	159	318	318	477	255	292	438	409
CPU time (min)	16	4	4	21	4	5	20	30	121	21	29	39	14

*Intel Xeon, 2.66 GHz, and 12 GB RAM.

the stage lengths can be treated as degrees of freedom allowing for an optimal choice of the location of the injection points. In contrast to this late discretization approach, where the solution of the spatial differential-algebraic reactor model is embedded in the optimization problem, Asteasuain and Brandolin[25] optimize the steady-state operation of a tubular reactor by means of an early discretization approach. Their method relies on spatial discretization of the tubular reactor model resulting in a nonlinear programming problem with a large number of nonlinear algebraic equality constraints, which is solved by the optimization toolbox of gPROMS. To represent a hydrogen injection, they add an extra source term to the mass and energy balances valid on the discretization interval starting at the injection point to approximate an impulse function. The lateral injection point has to be set a priori and cannot be considered as a degree of freedom.

The late multi-stage optimal control approach suggested here has several advantages. First, it allows for a precise consideration of the location of feed injection points which constitutes an important factor influencing the polymer quality. Furthermore, the shooting approach facilitates an accurate, error-controlled integration of the differential-algebraic polymerization model. Hence, the suggested novel problem formulation and solution algorithm outperforms previous methods with respect to robustness, solution accuracy and computational efficiency. In particular, Asteasuain and Brandolin[25] report that the solution of their optimization problem on a Pentium IV processor running at 3 GHz and using 1 GB RAM requires between 2 to 5 h of CPU time while our method solves a typical optimization problem, including the decision on lateral injection points as part of the optimization, in only 4 to 20 min on a comparable hardware, i.e., on an Intel Xeon running at 2.66 GHz and using 12 GB RAM.

Another early discretization approach has been recently proposed by Zavala and Biegler,[26] when targeting LDPE properties (MI and density) in tubular reactors while maintaining peak temperatures within protection zones. No attempt has been made to either target the whole MWD or to optimize the reactor length and lateral injection points. Their full discretization formulation is able to handle multi-point boundary conditions. Their steady-state reactor model contains about 130 ordinary differential equations and 500 algebraic equations. The optimization model, after full-discretization, covers around 13,000 constraints and 71 degrees of freedom.

Table 1 summarizes the computational effort for solving the optimization problems described in the next section for the series and parallel reactor configurations. The series configuration comprises four stages, eight decision variables (Eq. 10), 131 differential variables, 3369 algebraic variables, and 33 transition conditions between two adjacent stages. The parallel configuration consists of three stages, 14 decision variables (Eq. 11), 165 differential variables, 3513 algebraic variables, and 66 transition conditions between two adjacent stages.

Results and Discussion

Some optimizations runs are presented in this section to illustrate the implementation and the potential of the proposed approach for an industrial high density polyethylene reactor. For reasons of confidentiality, all data shown in the figures and tables have been normalized between 0 and 1. Examples 1 and 2 correspond to the series configuration (cf. Figure 1a), whereas Examples 3 and 4 refer to the parallel configuration (cf. Figure 1b).

Usually, in industrial practice the end-use properties are specified by the customer. A MWD complying with these specifications is obtained from laboratory tests (or from product/process knowledge). Some efforts have been made to develop models correlating end-use properties with the MWD.[2–7] If such models are incorporated in the process model, the end-use properties could be directly targeted by the optimization model. In the following case study, the target MWD is specified point-wise at selected molecular weights within a given tolerance (δ).

Figure 3 depicts the optimization procedure employed. The feasibility test refers to a least-squares optimization whose objective function is given by:

$$\Phi = \sum_{k=1}^{N} \left(wd_k - wd_k^o \right), \tag{15}$$

where wd_k^o is the target concentration of monomer incorporated to the polymer with chain length p_k. Furthermore, when solving optimization problems (13) and (14) at this first stage, the MWD is unconstrained to check which operating conditions allow to reach the target MWD closely. The feasibility of the optimal MWD is then evaluated at every collocation point. If all MWD samples lie within specification, the problem is feasible and economical optimization can be carried out to determine the best operating conditions. For the economical optimization, though, it is not necessary to constraint the MWD at all collocation points to reduce the complexity of the optimization problem as discussed above. However, if the MWD at some collocation point p_k violates the specification tolerance, a new optimization should be carried out with an additional constraint on wd_k at p_k to reach a feasible solution.

Alternatively, economical optimization could be performed without the proposed hierarchical approach depicted in Figure 3. If the polymerization system is unable to produce the target MWD, then the optimization will warn that a nonfeasible solution was found. However, the hierarchical approach proposed here allows for identifying how near to
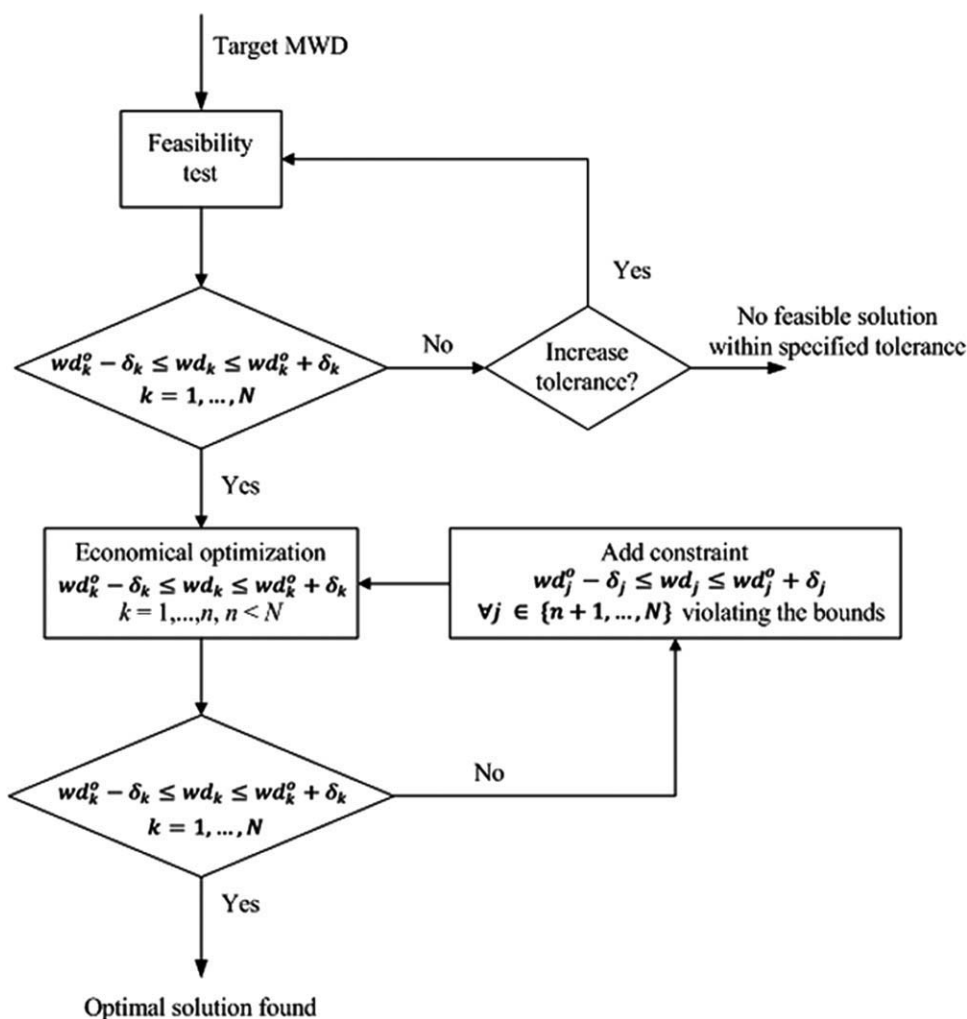
Figure 3. Optimization procedure.

the target MWD the process can operate. That makes the optimization strategy more robust and efficient.

Series configuration—Example 1

Figure 4 shows the MWD and average properties (MI and SE) of the polymer resin "Grade X," which should be designed within the tolerance $wd_k^o - \delta_k \leq wd_k \leq wd_k^o + \delta_k$,
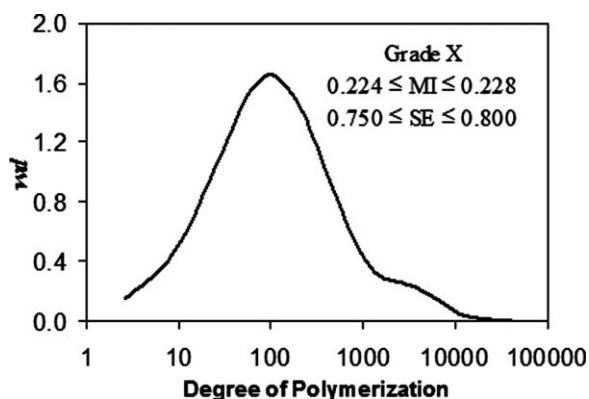
$k = 1,\ldots, N$, $\delta_k = 0.01$. Its MWD presents a tail at longer chains which is desirable for some end-use polymer properties. Attempting to target "Grade X" in Example 1, three

Figure 4. Target MWD for Example 1, "Grade X."

Table 2. Optimal Operating Conditions and Output Variables for Example 1

Type	Name	(1a)	(1b)	(1c)
Design variable	CAT	0.889	0.784	0.778
	M	0.748	0.732	0.711
	$H_{2,0}$	0.017	0.017	0.017
	T_{in}	0.732	0.797	0.861
	P_{in}	1.000	1.000	1.000
	W_t	0.400	0.431	0.540
	H_1	0.183	0.413	0.466
	z_1	0.597	0.929	0.912
Index variable	MI	0.224	0.208	0.224
	SE	0.750	0.740	0.750
Output variable	T_{out}	1.000	1.000	1.000
	P_{out}	0.500	0.500	0.500
	Q	0.975	0.961	0.961
	W_{PE}	0.568	0.553	0.568
	Revenue	0.641	0.632	0.641
	Cost	0.536	0.531	0.545
	Profit	0.105	0.101	0.096
CPU time*	(min)	15.6	3.4	4.0

*Intel Xeon 2.66 GHz and 12 GB RAM.
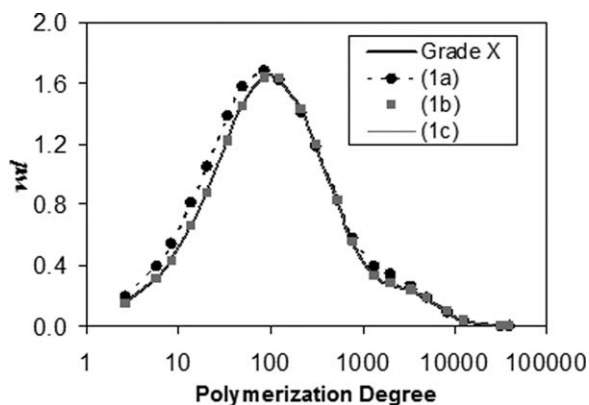
Figure 5. Target vs. optimal MWDs—Example 1.

Figure 6. Optimal MWD of Example 2: $0.268 \leq$ MI $\leq$ 0.273.

optimization runs are carried out; namely (1a) constraining MI and SE, (1b) constraining MWD and (1c) constraining MI, SE, and MWD.

The optimal operating conditions as well as the corresponding output variables are shown in Table 2 and the optimal MWDs are illustrated in Figure 5. In optimization (1a), despite MI and SE being the same as in the target polymer, a MWD results which is different from the target. Specifying only average properties does often not lead to the desired MWD. Hence, targeting of the complete MWD is necessary. To do so, it is not necessary to impose constraints on all N collocation points used to predict the MWD. According to our experience, if four collocation points are constrained, i.e., wd_4, wd_7, wd_{10}, wd_{15}, the optimal MWD agrees very well with the target MWD (Figure 5 (1b)). However, the MI and SE at the optimum are different from that of the target polymer (Table 2 (1b)). MI and SE measure the MWD's average and dispersion, respectively. These correlations are very sensitive, in particular, the MI correlation with respect to the average molecular weight. Therefore, a small change in the average and dispersion of the MWD results in a more pronounced change in MI and SE. The disagreement of the average properties therefore indicates that the optimal MWD is very similar, but not identical to the target distribution. Depending on the accuracy desired for the MWD and its average properties, constraints on wd_k might be
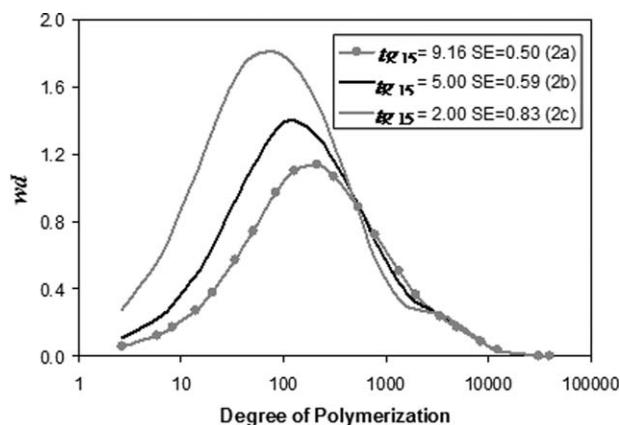
tightened and additional constraints on the MWD or on the MI and SE might be defined. In Example (1c), therefore, not only wd_k, but also MI and SE are constrained. The optimized results are shown in Table 2 (1c), and the MWD is illustrated in Figure 5 (1c). Finally, all the properties specified for the target polymer are satisfactorily achieved.

Series configuration—Example 2

As mentioned before, the presence of tails at high molecular weights may be desirable for some polymer end-use applications.[4] To this end, Example 2 illustrates how to design MWDs with a higher concentration of longer chains with constrained average molecular weight denoted by MI. This can be achieved by reducing the slope of the tangent tg (p_k) to the MWD at a specified chain length p_k. The values of tg (p_k) are computed by

$$tg(p_k) = \frac{wd_{k+1} - wd_k}{p_{k+1} - p_k} \quad (16)$$

where wd_k is given in Eq. 8 and p_k is the chain length at collocation point k. Therefore, tails can be obtained if tg (p_k) is added to the constraint vector **h** in Eq. 12.
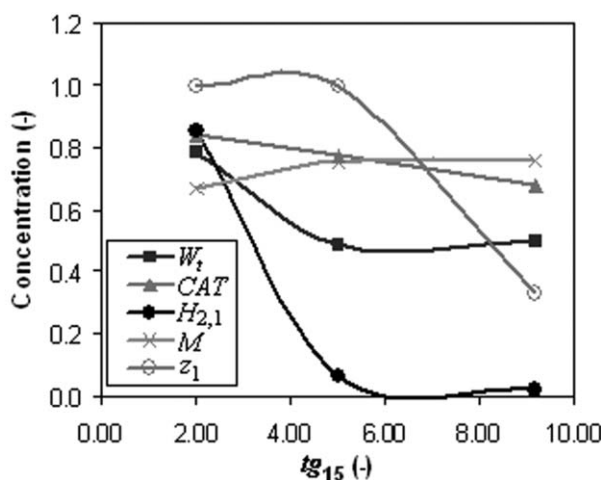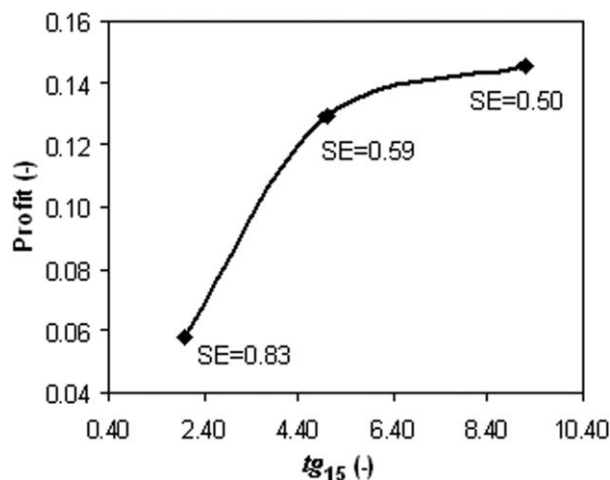

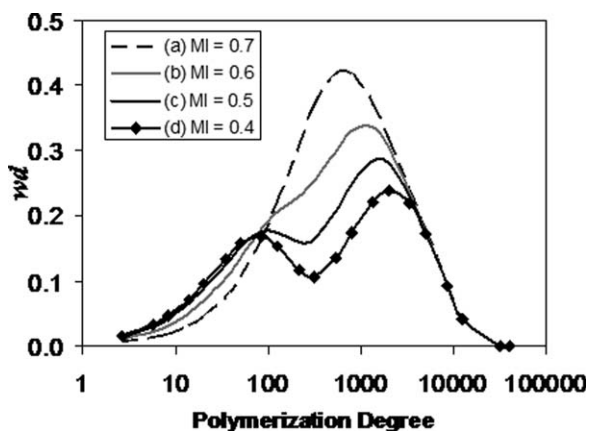**Figure 7. Profit (left) and inlet concentrations (right) vs. tg_{15} for $0.268 \leq$ MI $\leq$ 0.273.**

Figure 8. Optimal MWDs—Example 3.

If only MI is constrained by $0.268 \leq MI \leq 0.273$, the optimal MWD resembles a Gaussian distribution, as depicted in Figure 6 (dotted line). Attempting to obtain the tails at high molecular weights, two further optimizations are carried out with the constraint: $tg_{15} \leq 5$ and $tg_{15} \leq 2$. The optimal MWDs shown in Figure 6 present the desired tails at high molecular weights. The lower the tangent to the curve, the more pronounced the tail and therefore the higher the SE (polydispersity).

The optimal operating policies for the three optima are illustrated in Figure 7. The tails on the MWD are associated with higher catalyst inlet concentrations and consequently higher polydispersity (SE). Higher catalyst inlet concentrations enhance propagation reactions and thus increase temperature. In the first section of the reactor, the higher temperature increases the transfer reaction rates and then decreases the polymer molecular weight. On the other hand, as the reaction proceeds higher temperatures are reached, which lead to a deactivation of the catalytic sites. With the smaller number of active species in the final section of the reactor, the polymer molecular weight tends to increase (lower MI). Such different operating conditions yield a resin with higher SE.

Tradeoffs between catalyst (CAT), total flow rate (W_t) and monomer inlet concentrations (M) lead to lower costs for

increasing tg (p_k) (or lower SE) at nearly the same revenue, thus resulting in higher profit. It is also interesting to observe the lateral hydrogen injection point and its concentration effects on the tangent to the MWD. If the location of the lateral injection point is not an optimization degree of freedom, a sub-optimal operating condition might result. For more details about the phenomena taking place inside the reactor, the reader is referred to Pontes et al.[50]

Parallel configuration—Example 3

Due to intrinsic characteristics of tubular and stirred tank reactors, the former produces a polymer with high molecular weight, whereas the latter yields a lower molecular weight product. When both reactors are operated in series and the stirrer of the CSTR is switched off, there is some degree of mixing during polymer chain growth due to molecular diffusion. Therefore, despite the different characteristics of both reactors, the MWDs obtained are monomodal or at maximum present a tail at higher molecular weights. On the other hand, if the PFR and the CSTR are operated in parallel and if their products are mixed at the outlet, it might be possible to obtain a bimodal MWD. Bimodal polymer grades are highly specialized polymers which sell at higher prices than the ones specified in the previous examples (Eq. 9).[33]

Example 3 studies how MWD evolves for different average molecular weights but for the same polydispersity. Hence, a sequence of four optimizations is carried out with the following specifications for MI:

$$
\begin{align}
(3a) \quad & 0.071 \leq MI \leq 0.082, \\
(3b) \quad & 0.059 \leq MI \leq 0.071, \\
(3c) \quad & 0.047 \leq MI \leq 0.059, \\
(3d) \quad & 0.035 \leq MI \leq 0.047,
\end{align}
\tag{17}
$$

and $0.340 \leq SE \leq 0.380$ for SE in all cases above. The resulting optimal MWDs are illustrated in Figure 8. They vary from a monomodal to a typical bimodal MWD as MI decreases or molecular weight increases. Operational conditions as well as profit, polymer production rate (W_{PE}) and ratio of polymer
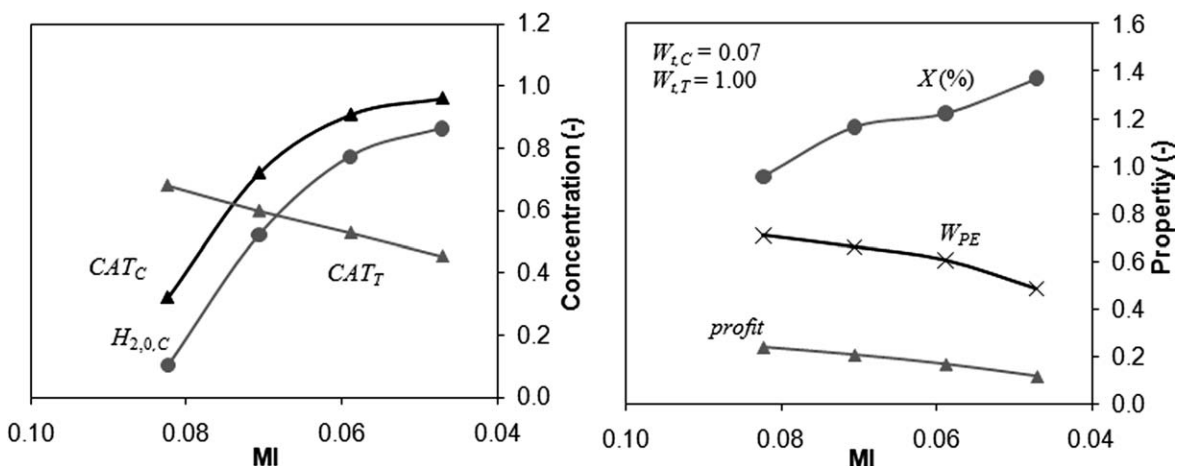

Figure 9. Inlet concentrations (left); profit, polymer production rate (W_{PE}) and ratio of polymer produced in CSTR (X)—Example 3.
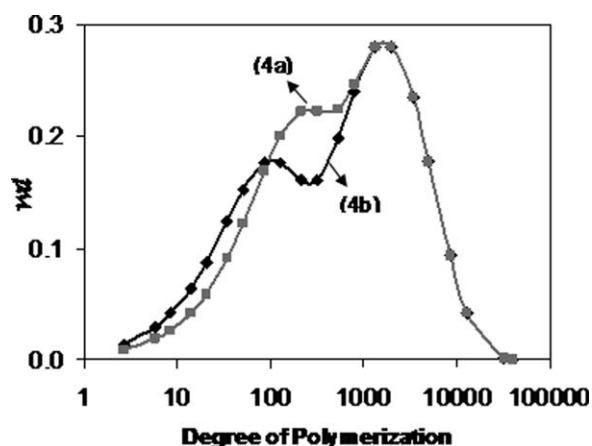
Figure 10. Optimal MWD for parallel configuration—Example 4(a,b).

produced in CSTR (X) are shown in Figure 9. For each reactor, all optimal flow rates are the same, but the CSTR operates almost at its lower flow rate limit, unlike the tubular reactor.

It is interesting to observe the antagonist behavior of the catalyst inlet concentration to each reactor in Figure 9. As mentioned before, lower catalyst concentration leads to longer polymeric chains, i.e., with lower MI. The hydrogen inlet concentration to PFR$_a$ is zero for all optimizations, also enhancing the formation of longer chains. Therefore, we can conclude that PFR$_a$ is responsible for the longer chains whereas the CSTR contributes to the smaller chains. As the ratio of polymer produced in the CSTR increases, the MWD tends to a bimodal distribution as observed in Figure 8.

Parallel configuration—Example 4

Once knowing MWD (3d) in Figure 8, for example, it is possible to target it by constraining the concentrations at only three collocation points: at the two peaks and at the minimum. On the other hand, if only the location of the two peaks is of interest, a bimodal distribution with peaks around

chain lengths p_{k1} and p_{k2} may be obtained when the constraints are imposed in the optimization problem, i.e., wd_{k_i} is a maximum because the concentration at p_{ki} is h_{ij} units greater than the concentration at j collocation points back and j collocation points forward:

$$wd_{k_i} - wd_{k_i-j} > h_{ij} \text{ and } wd_{k_i} - wd_{k_i+j} > h_{ij},$$
$$i = 1, 2, j = 1, 2, \ldots, \quad (18)$$

The parameter h_{ij} can further determine the height of the desired peak.

Figure 10 illustrates the optimal MWD for two different locations of the lower peak: (4a) $k_1 = 10$, $k_2 = 15$ and $j = 1$; (4b) $k_1 = 8$, $k_2 = 15$ and $j = 1$.

Table 3 gives the input conditions to each reactor as well as the output from the mixer. The main difference between operating conditions (4a) and (4b) is the higher monomer and catalyst inlet concentrations to the CSTR, increasing polymer conversion X in that reactor.

The optimal MWDs shown in Figure 10 have a more pronounced higher molecular weight peak because operating PFR$_a$ is more profitable than operating the CSTR. Another constraint might be additionally considered if a more pronounced lower molecular weight peak is desired. In this case, we request

$$wd_{k_1} - wd_{k_2} > d, \quad (19)$$

where d is the desired distance between the two peaks. To illustrate this, example (4c) takes example (4b) as starting point and adds constraint (19), with $d = 0.01$. As the economic objective leads to the lowest distance between the two peaks, it is not necessary to define an equality constraint and Eq. 19 is sufficient to achieve the desired distance between both peaks.

Figure 11 illustrates the optimal MWD for example (4c), the respective operating conditions are given in Table 3. The higher flow rate fed to the CSTR (W_t) increases the ratio of polymer produced in this reactor, i.e., 4.2% for Example (4c) vs. 1.3% for Example (4b). As mentioned before, stirring in the CSTR yields a polymer with lower molecular

Table 3. Optimal Conditions for Parallel Configuration—Example 4

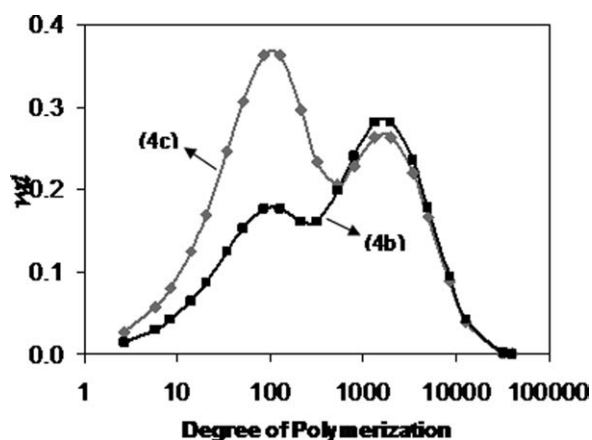|	(4a)		(4b)		(4c)	
	CSTR	PFR$_a$	CSTR	PFR$_a$	CSTR	PFR$_a$
CAT	0.907	0.517	0.879	0.518	0.962	0.518
M	0.235	0.717	0.125	0.718	0.179	0.708
H$_{2,0}$	0.651	0.000	0.699	0.000	1.000	0.000
W_t	0.067	1.000	0.067	1.000	0.148	1.000
W_s/H$_{2,1}$	0.667	0.000	0.009	0.000	0.009	0.000
	Mixer output		Mixer output		Mixer output	
MI	0.0600		0.0576		0.0647	
SE	0.3300		0.3400		0.4200	
W_{PE}	0.5480		0.5375		0.5590	
X	2.4300		1.3000		4.2000	
Profit	0.1622		0.1593		0.1486	

Figure 11. Optimal MWD for parallel configuration—Example 4(b,c).

weight; therefore, a higher peak around $p_{k1} = 10$ is observed in Example (4c). It is also interesting to note that hydrogen plays an important role when targeting a bimodal distribution since the chain transfer agent is used to control the MWD. No hydrogen is fed to the PFR, whereas the CSTR operates with a very high concentration, ensuring different molecular weights being produced in each reactor and then yielding the desired bimodal distribution.

Conclusions

This article presents a multi-stage optimization model and a shooting type solution method for determining optimal operating policies for the production of polyethylene resins with target quality specifications. It considers not only average properties but also the complete MWD because some end-use properties better correlate with the full distribution. The multi-reactor process comprises continuous stirred and tubular reactors that are modeled in steady state. The optimization problem encounters equality constraints which are differential-algebraic equations in the spatial coordinate such that a shooting method can be used for numerical solution. A complex multi-stage optimization problem is formulated and solved much more efficiently than by alternative methods employed previously. The results illustrate the need to design the whole MWD, as polymer resins with the same average properties may show different distributions. Furthermore, the shape of the distribution can be manipulated to produce resins with a known MWD, with tails in the MWD at higher degrees of polymerization or even to produce specialty polymer with a bimodal MWD. The tradeoff between catalyst and ethylene inlet concentrations has a great influence on the final profit profile. In addition, catalyst inlet concentration as well as hydrogen inlet concentration and its lateral injection point are identified to be important variables to control the shape of the MWD. The potential of the proposed approach also becomes evident through the excellent agreement between the target and the optimal MWD. Therefore, the optimization methodology developed here allows for significant opportunities for quality improvement and new product development while overcoming the uncertainties and high costs usually associated with industrial trial and error tests.

Acknowledgments

Notation

A = cross sectional area (m^2)
a = polyethylene sales price (€/kg)
b = unitary costs (€/kg)
b = coefficients
B = recycle stream mass flow rate (kg/s)
C = catalyst
$C*$ = activated catalyst
CC = co-catalyst
CCD = deactivated co-catalyst
CD = deactivated catalyst
C_i = component i concentration (kmol/m^3)

Cp = specific heat (J/kg K)
d = distance between two peaks of the MWD
D_0, D_{Ror}, D_F = constant coefficient
ΔH_p^o = enthalpy of reaction at the reference temperature (J/kmol)
$\mathbf{f}$ = vector of differential equations
F = mass flow rate (kg/s)
FZ = mass flow rate (kg/s)
$\mathbf{g}$ = vector of algebraic equations
$\mathbf{h}$ = vector of constraints at the outlet of PFR$_2$
h = height of MWD peak
$H_{2,0}$ = hydrogen concentration at main feed
$H_{2,1}$ = hydrogen concentration at lateral injection point
I = poison
J = number of PFR segments
$\mathbf{J}$ = vector of mapping conditions
k = stage number
k_p = rate constant for propagation
k_{fm} = rate constant for transfer with monomer
k_{fh} = rate constant for transfer with hydrogen
k_{fCC} = rate constant for transfer with co-catalyst
k_f = rate constant for spontaneous transfer
k_{tm} = rate constant for termination with monomer
k_{th} = rate constant for termination with hydrogen
k_{tCC} = rate constant for termination with co-catalyst
k_t = rate constant for spontaneous termination
l = length of a PFR segment
$\mathbf{lb}$ = vector of lower bounds
M = monomer
MI = polymer melt index
n = number of constrained collocation points
N = number of collocation points
dim = number of intervals on the domain
nh = order of Hahn polynomials
npt = total number of collocation points
$\mathbf{p}$ = vector of invariant parameters
p = collocation point
P = chain length domain
P = live polymer
PD = polydispersity;
P_{in} = inlet pressure
P_{out} = outlet pressure
X = conversion
r = reaction rate
R = number of CSTR ideal compartments
Rot = agitator rotation
SE = polymer stress exponent
T = temperature
T_{in} = inlet temperature
T_{out} = outlet temperature
tg = tangent to the MWD
U = dead polymer
$\mathbf{u}$ = vector of decision variables
$\mathbf{ub}$ = vector of upper bounds
W = mass flow rate (Kg/s)
wd = concentration of monomer incorporated into polymer
W_{PE} = polymer production rate
W_s = side feed
W_t = total mass flow rate
$\mathbf{x}$ = vector of differential state variables
$\mathbf{y}$ = vector of algebraic state variables
z = axial coordinate
z_1 = lateral hydrogen injection point

Superscript

$ofcc$ = order of transfer with co-catalyst reaction
ofh = order of transfer with hydrogen reaction
$otcc$ = order of termination with co-catalyst reaction
oth = order of termination with hydrogen reaction

Subscript

j = segment of PFR
k = index of collocation point

M = monomer
p = polymer chain length
r = CSTR ideal zone
U = dead polymer

Greek letters

α = empirical constant
β = empirical constant
ϕ = linearly independent functions
γ = empirical constant
λ_k = dead polymer moment of order k
ρ = medium specific mass (kg/m^3)
δ = tolerance for MWD specification

Literature Cited

1. Kiparissides C. Polymerization reactor modeling: a review of recent developments and future directions. *Chem Eng Sci*. 1996;51:1637–1659.
2. Costa MCB, Jardini AL, Lima NMN, Embiruçu M, Wolf Maciel MR, Maciel Filho R. Empirical models for end-use properties prediction: application to injection molding of some polyethylene resins. *J Appl Polym Sci (Print)*. 2009;114:3780–3792.
3. Latado A, Embiruçu M, Mattos A, Pinto JC. Modeling of end-use properties of poly(propylene/ethylene) resins. *Polym Test*. 2001;20:419–439.
4. Ariawan AB, Hatzikiriakos SG, Goyal SK, Hay H. Effects of molecular structure on the rheology and processability of blow-molding high-density polyethylene resins. *Adv Polym Technol*. 2001;20:1–13.
5. Hinchliffe M, Montague G, Willis M, Burke A. Hybrid approach to modeling an industrial polyethylene process. *AIChE J*. 2003;49:3127–3137.
6. Nele M, Latado A, Pinto JC. Correlating polymer parameters to the entire molecular weight distribution: application to the melt index. *Macromol Mater Eng*. 2006;291:272–278.
7. Zahedi M, Ahmadi M, Nekoomanesh M. Influence of molecular weight distribution on flow properties of commercial polyolefins. *J Appl Polym Sci*. 2008;108:3565–3571.
8. Jang SS, Tan DM, Wie IJ. Optimal operations of semi batch solution polymerization of acrylamide with molecular distribution as constraints. *J Appl Polym Sci*. 1993;50:1959–1967.
9. Sundaram BS, Upreti SR, Lohi A. Optimal control of batch MMA polymerization with specified time, monomer conversion, and average polymer molecular weights. *Macromol Theory Simul*. 2005;14:374–386.
10. Zhang JA. Reliable neural network model based optimal control strategy for a batch polymerization reactor. *Ind Eng Chem Res*. 2004;43:1030–1038.
11. Curteanu S, Leon F, Gâlea D. Alternatives for multiobjective optimization of a polymerization process. *J Appl Polym Sci*. 2006;100:3680–3695.
12. Ahn AO, Chang SC, Rhee HK. Application of optimal temperature trajectory to batch polymerization reactor. *J Appl Polym Sci*. 1998;69:59–68.
13. Crowley TJ, Choi KY. Discrete optimal control of molecular weight distribution in a batch free radical polymerization process. *Ind Eng Chem Res*. 1997;36:3676–3684.
14. Crowley TJ, Choi KY. Calculation of molecular weight distribution from molecular weight moments in free radical polymerization. *Ind Eng Chem Res*. 1997;36:1419–1423.
15. Crowley TJ, Choi KY. Control of molecular weight distribution and tensile strength in a free radical polymerization process. *J Appl Polym Sci*. 1998;70:1017–1026.
16. Sayer C, Araujo PHH, Arzamendi G, Asua JM, Lima EL, Pinto JC. Modeling molecular weight distribution in emulsion polymerization reactions with transfer to polymer. *J Polym Sci Part A: Polym Chem*. 2001;39:3513–3528.
17. Kiparissides C, Seferlis P, Mourikas G, Morris AJ. Online optimizing control of molecular weight properties in batch free-radical polymerization reactors. *Ind Eng Chem Res*. 2002;20:6120–6131.
18. Saliakas V, Chatzidoukas C, Krallis A, Meimaroglou D, Kiparissides C. Dynamic optimization of molecular weight distribution using orthogonal collocation on finite elements and fixed pivot methods: an experimental and theoretical investigation. *Macromol React Eng*. 2007;1:119–136.
19. Vicente M, Sayer C, Leiza JR, Arzamendi G, Lima EL, Pinto JC, Asuaa JM. Dynamic optimization of non-linear emulsion copolymerization systems. Open-loop control of composition and molecular weight distribution. *Chem Eng J*. 2002;85:339–349.
20. Asteasuain M, Soares M, Lenzi MK, Cunningham M, Sarmoria C, Pinto JC, Brandolin A. "Living" free radical polymerization in tubular reactors. I. Modeling of the complete molecular weight distribution using probability generating functions. *Macromol React Eng*. 2007;1:622–634.
21. Asteasuain M, Soares M, Lenzi MK, Hutchinson RA, Cunningham M, Brandolin A, Pinto JC, Sarmoria C. "Living" radical polymerization in tubular reactors, 2 – process optimization for tailor-made molecular weight distributions. *Macromol React Eng*. 2008;2:414–421.
22. Brandolin A, Valles EM, Farber JN. High pressure tubular reactors for ethylene. Polymerization optimization aspects. *Polym Eng Sci*. 1991;31:381–390.
23. Asteasuain M, Ugrin PE, Lacunza MH, Brandolin A. Effect of multiple feedings in the operation of a high-pressure polymerization reactor for ethylene polymerization. *Polym React Eng*. 2001;9:163–182.
24. Cervantes A, Tonelli S, Brandolin A, Bandoni A, Biegler L. Large-scale dynamic optimization of a low density polyethylene plant. *Comput Chem Eng*. 2002;24:983–989.
25. Asteasuain M, Brandolin A. Modeling and optimization of a high-pressure ethylene polymerization reactor using gPROMS. *Comput Chem Eng*. 2008;32:396–408.
26. Zavala VM, Biegler LT. Large-scale nonlinear programming strategies for the operation of ldpe tubular reactors. 18th European Symposium on Computer Aided Process Engineering—ESCAPE 18, Lyon, France. 2008.
27. Kiparissides C, Verros G, MacGregor JF. Mathematical modeling, optimization, and quality control of high-pressure ethylene polymerization reactors. *Polym Rev*. 1993;33:437–527.
28. Kiparissides C, Verrosa G, Pertsinidisa A. On-line optimization of a high-pressure low-density polyethylene tubular reactor. *Chem Eng Sci*. 1994;49:5011–5024.
29. McAuley KB, MacGregor JF. Optimal grade transitions in a gas-phase polyethylene reactor. *AICHE J*. 1992;38:1564–1576.
30. Chatzidoukas C, Perkins JD, Pistikopoulos EN, Kiparissides C. Optimal grade transition and selection of closed-loop controllers in a gas-phase olefin polymerization fluidized bed reactor. *Chem Eng Sci*. 2003;58:3643–3658.
31. Chatzidoukas C, Pistikopoulos S, Kiparissides C. A hierarchical optimization approach to optimal production scheduling in an industrial continuous olefin polymerization reactor. *Macromol React Eng*. 2003;3:36–46.
32. Embiruçu M, Fontes C. Multi-rate multivariable generalized predictive control and its application to a slurry reactor for ethylene polymerization. *Chem Eng Sci*. 2006;61:5754–5767.
33. Pontes KV, Maciel R, Embiruçu M, Hartwich A, Marquardt W. Optimal operating policies for tailored linear polyethylene resins production. *AIChE J*. 2008;54:2346–2365.
34. Embiruçu M, Lima EL, Pinto JC. Continuous soluble Ziegler-Natta ethylene polymerizations in reactor trains. I. Mathematical modeling. *J Appl Polym Sci*. 2000;77:1574–1590.
35. Vieira RAM, Embiruçu M, Sayer C, Pinto JC, Lima EL. Control strategies for complex chemical processes. Applications in polymerization processes. *Comput Chem Eng*. 2003;27:1307–1327.
36. Pinto JC, Oliveira AM Jr, Lima EL, Embiruçu M. Data Reconciliation in a Ziegler-Natta ethylene polymerization. *Dechema-Monographien*. 2004;138:531–535.
37. Embiruçu M, Prata DM, Lima EL, Pinto JC. Continuous soluble Ziegler-Natta ethylene polymerizations in reactor trains, 2—estimation of kinetic parameters from industrial data. *Macromol React Eng*. 2008;2:142–160.
38. Embiruçu M, Pontes KV, Lima EL, Pinto JC. Continuous soluble Ziegler-Natta ethylene polymerizations in reactor trains, 3—influence of operating conditions upon process performance. *Macromol React Eng*. 2008;2:161–175.

39. Pontes KV, Cavalcanti M, Maciel Filho R, Embiruçu M. Modeling and simulation of ethylene and 1-butene copolymerization in solution with a Ziegler-Natta Catalyst. *Int J Chem React Eng*. 2010; 8:A7.

40. Pontes KV, Maciel R, Embiruçu M. An approach for complete molecular weight distribution calculation: application in ethylene coordination polymerization. *J Appl Polym Sci*. 2008;109:2176–2186.

41. Brandolin A, Sarmonia C. Prediction of molecular weight distributions by probability generating functions. Application to industrial autoclave reactors for high pressure polymerization of ethylene and ethylene-vinyl acetate. *Polym Eng Sci*. 2001;41:1413–1426.

42. Villadsen J, Michelsen ML. *Solution of Differential Equation Models by Polynomial Approximation*. Englewood Cliffs, NJ: Prentice Hall, 1978:446 p.

43. Canu P, Ray WH. Discrete weighted residual methods applied to polymerization reactors. *Comput Chem Eng*. 1991;15:549–564.

44. Neumann CP. Discrete weighted residual methods: a survey. *Int J Syst Sci*. 1977;8:985–1007.

45. Nele M, Sayer C, Pinto JC. Computation of molecular weight distributions by polynomial approximation with complete adaptation procedures. *Macromol Theory Simul*. 1999;8:199–213.

46. Wulkow M, Deuflhard P. *Towards an efficient computational treatment of heterogeneous polymer reactions*. In: Fatunla SO, editor. *Computational Ordinary Differential Equations*. Ibadan: University Press Plc, 1992: 287:306.

47. O'Driscoll KF, Ponnuswamy SR. Optimization of a batch polymerization reactor at the final stage of conversion. II. Molecular weight constraint. *J Appl Polym Sci*. 1990;39:1299–1308.

48. Oliveira AT, Biscaia EC, Pinto JC. Optimization of batch solution polymerizations: simulation studies using an inhibitor and a chain-tansfer agent. *J Appl Polym Sci*. 1998;69:1137–1152.

49. Tieu D, Cluett R, Penlidis A. Optimization of polymerization reactor operation: review and case studies with the end-point collocation method. *Polym React Eng*. 1994;2:275–313.

50. Pontes KV, Maciel R, Embiruçu M. Process analysis and optimization mapping through design of experiments and its application to a polymerization process. PPS 23—The Polymer Processing Society 23rd Annual Meeting, Salvador, 2007.

51. Brendel M, Oldenburg J, Schlegel M, Stockmann K. *DyOS user manual, relase 2.1. Lehrstuhl für Prozesstechnik*, RWTH Aachen, Aachen, Germany, 2002.

52. Oldenburg J, Marquardt W. Disjunctive modeling for optimal control of hybrid dynamic systems. *Comput Chem Eng*. 2007;32:2346.

53. Schlegel M, Stockman K, Binder T, Marquardt W. Dynamic optimization using adaptative control vector parametrization. *Comput Chem Eng*. 2005;29:1731–1751.

Appendix

This appendix summarizes the kinetic mechanism, the process model and the polymer property models developed in previous studies.[32–39]

The catalyst is a mixture of vanadium and titanium based catalysts, activated by triethyl aluminum. The kinetic mechanism is described in Table A1.

The reactor configuration comprises tubular and stirred tank reactors modeled by the equations in Tables A2 and A3, respectively. The first PFR is divided into J segments with PFR characteristics, where the starting point of compartment j is located at the lateral mass injection points (F_j). The nonideal CSTR is represented by a sequence of R ideally mixed compartments in series with backmixing (B) between two adjacent compartments to represent the mixing inside the reactor. The side feeds to the CSTR are represented by FZ_r.

Some average polymer properties are related to the MWD to be used in the optimization of product quality. Those properties include the MI,

$$\mathrm{MI} = \alpha_1 \cdot \left(\overline{\mathrm{MW}}_w\right)^{-\beta_1}, \tag{A1}$$

and the SE,

Table A1. Kinetic Mechanism of Ethylene Copolymerization by Coordination

Reaction	Rate
Activation	
$C_n + CC \rightarrow C^*_n$	$k_{f,n} \cdot [C_n] \cdot [CC]$
Poisoning by impurities	
$I_{CC} + CC \rightarrow CCD$	$k_{ICC} \cdot [I_{CC}] \cdot [CC]$
$I_{C^*} + C^*_n \rightarrow CD_n$	$k_{IC} \cdot [I_{C^*}] \cdot [C^*_n]$
Initiation	
$C^*_n + M \rightarrow P_{1,n}$	$k_{i,n} \cdot [C^*_n] \cdot [M]$
Propagation	
$P_{i,n} + M \xrightarrow{k_{p,n}} P_{i+1,n}$	$k_{p,n} \cdot [P_{i,n}]$ 7middot; $[M]$
Spontaneous Deactivation	
$C^*_n \rightarrow CD$	$k_{d,n} \cdot [C^*_n]$
Transfer	
$P_{i,n} + M \xrightarrow{k_{fm,n}} P_{1,n} + U_i$	$k_{fm,n} \cdot [P_{i,n}] \cdot [M]$
$P_{i,n} + H_2 \xrightarrow{k_{fh,n}} C^*_n + U_i$	$k_{fh,n} \cdot [P_{i,n}] \cdot [H_2]$
$P_{i,n} + CC \xrightarrow{k_{fCC,n}} C^*_n + U_i$	$k_{fCC,n} \cdot [P_{i,n}] \cdot [CC]$
$P_{i,n} \xrightarrow{k_{f,n}} C^*_n + U_i$	$k_{f,n} \cdot [P_{i,n}]$
Termination	
$P_{i,n} + M \xrightarrow{k_{tm,n}} CD + U_i$	$k_{tm,n} \cdot [P_{i,n}] \cdot [M]$
$P_{i,n} + H_2 \xrightarrow{k_{th,n}} CD + U_i$	$k_{th,n} \cdot [P_{i,n}] \cdot [H_2]$
$P_{i,n} + CC \xrightarrow{k_{tCC,n}} CD + U_i$	$k_{tCC,n} \cdot [P_{i,n}] \cdot [CC]$
$P_{i,n} \xrightarrow{k_{t,n}} CD + U_i$	$k_{t,n} \cdot [P_{i,n}]$

Table A2. Mathematical Model of the PFR Compartments

Mass balance
$$W_{j+1} = F_{j+1} + W_j \quad j = 1,2,\ldots,J-1,$$
$$\frac{1}{A} \cdot \frac{dW_j}{dzj} = 0 \Rightarrow W_j = \text{constant},$$
$$\frac{dC_{i,j}}{dz_j} = \frac{C_{i,j}}{\rho_j} \cdot \frac{d\rho_j}{dz_j} + r_{i,j} \cdot \frac{A \cdot \rho_j}{W_j}, \quad i = 1,\ldots,nc, \quad z_j \in (0, l_j],$$

Energy balance
$$Cp_j \cdot \frac{W_j}{A} \cdot \frac{dT_j}{dz_j} = -r_{p,r} \cdot \left(\Delta H_p^o + MW_M \cdot \int_o^r (Cp_U - Cp_M) dT \right),$$

Boundary conditions
$$C_{i,j}(z_j = 0) = C_{0,i,j}, \rho_j(z_j = 0) = \rho_{0,j}, T_j(z_j = 0) = T_{0,j}.$$

Table A3. Mathematical Model of the Nonideal CSTR

Mass balance
$$W_{r-1} + FZ_r + B_{r+1} - B_r - W_r = 0 \quad r = 1,\ldots R,$$
$$\frac{W_{r-1} \cdot C_{i,r-1}}{\rho_{r-1}} + \frac{FZ_r \cdot C_{i,r}}{\rho_{FZ_r}} + \frac{B_{r+1} \cdot C_{i,r+1}}{\rho_{r+1}} - \frac{(B_r + W_r) \cdot C_{i,r}}{\rho_r} + V_r \cdot r_{i,r} = 0 \quad i = 1,\ldots,nc,$$
$$B_1 = 0, B_{R+1} = 0, W_P = W_0$$

Energy balance
$$\sum_{i=1}^{nin} W_i \cdot \int_r^i Cp_i dT = -V_r \cdot r_{p,r} \cdot \left(\Delta H_p^o + MW_M \cdot \int_0^r (Cp_U - Cp_M) dT \right),$$

Backmixing model
$$B_r = \frac{k \cdot \rho_r V_r}{\mu_r} \cdot \left(D_{0,r} + D_{Rot,r} \cdot Rot + D_{F,r} \cdot FZ_r \cdot \left(\sum_{r=1}^{nr} FZ_r + W_0 \right)^{-1} \right)$$

$$\mathrm{SE} = \frac{1}{\alpha_2 + \gamma_2 \cdot \exp(-\beta_2 \cdot PD)}, \tag{A2}$$

where α_i, β_I, and γ_i are empirical constants determined by Embiruçu et al.[34]

The conversion and the polymer production rate are computed from

$$X = 100 \cdot \frac{\lambda_1}{C_M + \lambda_1} \tag{A3}$$

and

$$W_{PE} = \frac{W}{\rho} \cdot \lambda_1 \cdot MW_M \tag{A4}$$

respectively, where C_M is the monomer concentration, λ_1 is the first order dead polymer moment, W the total mass flow rate, MW_M is the monomer molecular weight and ρ the mixture density.